Available online at www.sciencedirect.com
SCIENCE DIRECT®
Chemical Physics Letters 401 (2005) 522–528
CHEMICAL PHYSICS LETTERS
www.elsevier.com/locate/cplett

Systematic inclusion of defects in pure carbon single-wall nanotubes and their effect on the Raman D-band

A.C. Dillon *,[1], P.A. Parilla [1], J.L. Alleman, T. Gennett, K.M. Jones, M.J. Heben

National Renewable Energy Laboratory, 1617 Cole Blvd., Golden, CO 80401, USA

Received 9 February 2004; in final form 23 September 2004
Available online 15 December 2004

Abstract

The Raman D-band feature (~1350 cm^{-1}) is examined with 2.54 eV excitation for pure bulk carbon single-wall nanotube samples before and after treatments that increase defect densities. Upon employing mass-transport-limited oxidation to introduce defects, the D-band intensity increases approximately linearly with reaction time. A relatively constant ratio of the D-band intensity and the major tangential G-band intensity (D/G) is observed for the purified samples examined at 2.54 and 1.96 eV suggesting a characteristic number of defects is introduced for given synthesis and purification processes. The D/G ratio is ~1/190 and 1/40 for excitation at 2.54 and 1.96 eV, respectively.

1. Introduction

Raman spectroscopy has been a very powerful tool for elucidating the electronic and vibrational structure of single-wall carbon nanotubes (SWNTs) [1]. The most striking features in the first-order Raman spectra are the low-frequency, diameter-dependent, radial breathing (RB) modes with A_1 symmetry (below 400 cm^{-1}), and the tangential 'G'-bands (1500–1650 cm^{-1}) consisting of six components with A_1, E_1, and E_2 symmetries arising from the curvature-induced splitting of the E_{2g} mode of graphite [2]. The chirality-dependent van Hove singularities in the electronic density of states [3] lead to resonance Raman effects [2,4,5]. Varying the Raman excitation energy (E_{laser}) probes different tubes of specific diameter and chirality. Pronounced resonances occur when the incoming or scattered photon energy exactly matches an electronic absorption transition at the van Hove singularities. When the resonance condition is exactly satisfied, intensity enhancements of a factor of 1000 may be observed [6].

Numerous theoretical efforts have focused on the properties of the tangential bands and the RB modes, and these main features can be well understood by considering only the properties of a single, perfect, infinite nanotube [1,3,4]. However, like other sp^2-hybridized carbons, SWNTs may also display a disorder-induced band (D-band) with a frequency between ~1250 and 1450 cm^{-1}, depending on E_{laser} [7]. The D-band has been attributed to an A-symmetry mode that is only activated by a loss of translational symmetry due to defects. Calculations indicate that virtually no intensity is expected for infinite, defect-free SWNTs [8]. However, significant SWNT Raman D-band intensity has been experimentally observed and analyzed. For example, Duesberg et al. [9] studied the polarization dependence of the Raman D-band from isolated SWNTs localized onto glass substrates by adsorption from aqueous solution. A maximum intensity for the D-band, as well as for all other SWNT modes, was observed when the nanotubes were aligned parallel to the polarization of the incident and scattered laser light. Due to the absence

* Corresponding author.
E-mail address: adillon@nrel.gov (A.C. Dillon).
[1] Both authors contributed equally.

0009-2614/$ - see front matter © 2004 Elsevier B.V. All rights reserved.
doi:10.1016/j.cplett.2004.11.104

of significant carbon impurities and the measured orientation dependence, the D-band signal was concluded to be a feature of the SWNTs and attributed to the presence of defects, bending, or finite-size effects [9]. Pimenta et al. [10] studied the D-band properties of isolated tubes grown by chemical vapor deposition and observed narrow signals with frequencies that decreased with decreasing tube diameter. The intensity of the D-band was observed to be random again suggesting dependence on unresolved extrinsic characteristics such as defect densities and finite tube lengths [10].

The D-band frequency is highly dispersive and increases with increasing laser excitation energy by $\sim$50 cm^{-1}/eV [7]. This dispersive nature of the D-band Raman spectra [6] as well as discrepancy between the D-band Stokes and anti-Stokes frequencies [11] have been explained recently by a double resonance process. The double resonance effect occurs when both the scattered intermediate state and the initial (or final) state are actual electronic states [12,13]. For the SWNT D-band, the double resonant process results in two different phonon frequencies suggesting that the observed spectra should be fit by two Lorenzians [6]. However, a detailed analysis of the SWNT Raman D-band fine structure has been recently provided [14,15]. Employing double resonant theory, the authors show that the SWNT D-band is characterized by a sharp main band of highest intensity and more than one broad sub-band of lower intensity. The high intensity main band originates from a 'triple' resonance effect where, in addition to the double resonance of the normal D-band, the incoming or scattered photon energy is also matched to a van Hove singularity. The lower intensity sub-bands result from the multiple ways double resonance can occur for a particular tube. When the double and triple resonances are taken into account for a polydisperse sample, very good agreement between calculated and experimental frequencies and intensities for both the main D-band and the sub-bands is observed [14,15].

Based on this new understanding for the origin of the D-band in SWNTs, the following conclusions are relevant for experimental observation of the D-band. (1) Defects allow the inelastic scattering needed for the single-phonon, double or triple resonance effects. The intensity of the observed SWNT D-band will therefore be proportional to the density of defects [16]. This conclusion was previously known before the new theory and is consistent with previous experimental data, but now the role of the defects are better understood. (2) Contribution to the main high intensity D-band peak are dominated by nanotubes that have van Hove singularities near the incoming or scattered photon energies [14,15]. Thus, for a given laser energy, the D-band signal originates from a subset of the nanotubes in a sample, and this applies similarly to the RB and G-bands [6]. Tubes that are resonant with the incoming laser light will all contribute to the RB, D-and G-bands. Tubes that are resonant with the scattered light may only contribute to a subset that depends on the resonance 'window'. This window has been estimated to be within a small energy range between 100 and 20 meV [6]. Given that the energy difference between the D and G bands is small ($\sim$25 meV), it is expected that the majority of the tubes contributing to the D band will also contribute to the G band and vice versa. It can thus be concluded that looking at the D/G intensity ratio will provide a meaningful measurement since the signals are coming from approximately the same tubes.

In this study, a dominant sharp SWNT D-band feature is observed for bulk SWNT materials at 1360 cm^{-1} for E_{laser} = 2.54 eV. Broader side bands with decreased intensity are observed at 1330, 1390 and 1423 cm^{-1}. These characteristic SWNT D-band features are only observed for purified materials that are virtually free from non-nanotube carbon impurities, and their intensities are approximately two orders of magnitude less than the intensity of the strongest G-band feature (E_{laser} = 2.54 eV). It is likely that defects are introduced during the purification process thereby activating the SWNT D-band intensity. In a previous study by Bahr et al., the SWNT D-band was observed to broaden, and the intensity increased to nearly that of the G-band when approximately 1/20 carbons in the SWNT were functionalized. Absorption spectra of the functionalized materials indicated a significant electronic perturbation of the nanotubes and a disruption of the extended π network [17]. Here, we demonstrate that by employing a gentle mass-transport-limited oxidation reaction to introduce defects, the intensity of the dominant Raman D-band is observed to increase only slightly (up to $\sim$2 times) and approximately linearly with reaction time. Furthermore, the SWNT D-band remains narrow until the tubes are significantly damaged and converted to non-nanotube disordered carbons. These experimental results confirm that defect introduction activates the SWNT D-band intensity as expected from theory [8,12,14]. Also, and somewhat surprisingly, for purified SWNT samples a roughly constant D/G intensity ratio was observed to be $\sim$1/190 and $\sim$1/40 for excitation at 2.54 and 1.96 eV, respectively. The findings suggest that the synthesis and purification techniques employed here reproducibly introduce a roughly constant number of defects.

2. Experimental

SWNT materials were produced by laser vaporization from graphite targets doped with 0.6 at% each of Co and Ni in a 1200 °C oven in a 500 torr Ar ambient using either a Nd:YAG (1064 nm) or an Alexandrite (755 nm) laser operating in a free-running mode. The

samples were purified by refluxing for 16 h in dilute (3.0 M) nitric acid and heating in air to 550 °C for 30 min, as previously described [18]. When care is taken to remain in a vaporization regime during synthesis, such that appreciable graphitic target material is not incorporated into the raw SWNT material [19], very high purity materials may be obtained with this simple purification process. A combination of thermal gravimetric analysis (TGA), inductively coupled plasma spectroscopy (ICP), and transmission electron microscopy (TEM) revealed that the resultant SWNT samples are close to 98 wt% pure. Weight analyses, TEM, and Raman studies performed at various stages of purification show that very few of the SWNTs are consumed during the reflux or oxidation processes [18] indicating that the as-synthesized laser materials are relatively un-reactive presumably due to low defect densities.

In order to slowly introduce defects, the samples were heated to temperatures between 1500 and 1650 °C inside a resistively heated tantalum foil. The chamber pressure rose to $\leqslant 10^{-5}$ torr during heating due to the intense thermal radiation and the accompanying desorption of water from the chamber walls. Temperatures were measured with both thermocouples and optical pyrometry. TEM was employed to evaluate the material before and after high temperature treatments. Samples were prepared for TEM by suspending ~0.2 mg of the material in 10 ml of acetone. The solutions were sonicated for 5 min, and ~6 drops were placed on Ted Pella Ultrathin Carbon Type-A 400 mesh grids. Images were obtained on a Phillips CM-30 TEM/STEM operating at 200 kV with a 50 μm objective aperture for improved contrast.

Raman spectroscopy was performed using 2.54 eV (488 nm) and 1.96 eV (632.8 nm) laser excitations. The back-scattered light was analyzed with a Jobin Yvon 270M spectrometer equipped with a liquid-nitrogen-cooled Spectrum One CCD and holographic notch filters. A Nikon 55 mm camera lens was employed both to focus the beam on the sample to an ~0.25 mm^2 spot and to collect the Raman scattered light. Averaging three 30 s scans was sufficient to obtain high intensity, well-resolved Raman spectra.

The dominant D-band peaks were analyzed by fitting the Poisson-weighted data to a single Lorentzian peak on top of a baseline for E_{laser} = 2.54 eV. Sufficient separation or significantly low intensity of the D-band subbands allowed for an accurate analysis with a single Lorentzian. Analysis for the main peak of the G-band was obtained by directly calculating the data for the maximum intensity and FWHM after subtracting a baseline intensity again using Poisson statistics for the uncertainty analysis (E_{laser} = 2.54 eV). For Raman excitation at 1.96 eV, analysis of both the main peak of the G-band and the D-band was obtained by directly calculating the data for the maximum intensity and FWHM after subtracting the baseline intensity. (At 1.96 eV, the main D-band feature had a significantly higher intensity and was very well resolved from the side bands.) The intensity of the D-band was examined by comparing the D/G ratios within a given spectrum. This approach accounts for variations in the sample surface roughness, the collection efficiency of the optics, and other extrinsic concerns which can cause the absolute Raman signals to vary in intensity by as much as 50% even for identical samples.

3. Results and discussion

Fig. 1 shows the Raman D-band spectra for excitation at 2.54 eV of both crude and purified (~98 wt% SWNTs) Alexandrite-generated material produced at a laser intensity of ~45 W/cm^2. The D-band of the crude material (1351 cm^{-1}) is quite broad with a full-width-at-half-maximum (FWHM) of ~42 cm^{-1}. This broad spectral feature in the crude materials is attributed to a convolution of the D-bands of non-nanotube carbon impurities including nanocrystalline graphite and amorphous carbon as well as any defective SWNTs present following this laser synthesis process. For 2.54 eV excitation, the FWHMs of the D-bands of nanocrystalline graphite and amorphous carbon are typically ~86 and 57 cm^{-1}, respectively [20]. Once the disordered carbon impurities are removed via purification, a sharp dominant D-band feature with a FWHM of ~17 cm^{-1} is observed at 1360 cm^{-1}. Broader features having much less intensity appear at 1390 and 1423 cm^{-1}, and a small shoulder is apparent at 1330 cm^{-1}. The SWNT D-band spectral features are similar to those observed previously for Raman excitation of 2.59 eV [15]. However, the dominant feature observed here at 1360 cm^{-1} is sharper

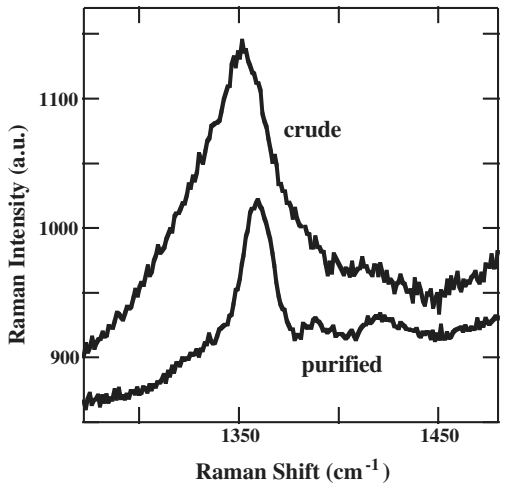

Fig. 1. Raman spectra taken with 2.54 eV excitation of as-synthesized and purified Alexandrite laser-generated material.

and better resolved from the sub-bands. Still the relatively narrow SWNT D-band observed in Fig. 1 is broader than the smallest D-band width ($\sim$6 cm^{-1}) previously observed for isolated SWNTs [10]. This is consistent with the fact that polydispersity in SWNT diameters is expected to lead to SWNT D-bands at different frequencies [10,15] and, therefore, an ensemble broadening of the observed signal. At 2.54 eV, the RB modes originate from tubes with diameters in the range between 1.2 and 1.5 nm [21,22].

Qualitatively, it is reasonable to expect a narrower D-band for purified SWNTs than for disordered carbon impurities because the number of atomic configurations and types of defects that could render the SWNT disorder mode Raman active are limited by the inherent SWNT structure. Since the FWHM of the SWNT D-band is much narrower than the D-bands of other disordered carbons, measuring the width of the Raman D-band may be employed to show that SWNT samples are relatively free from carbon impurities. It must be strongly emphasized, however, that the SWNT D-band width will vary both with nanotube diameter distribution and Raman laser excitation, so the Raman D-band FWHM of high purity samples must be obtained for various synthesis techniques (generating different diameter distributions) and at specific Raman excitations before employing Raman spectroscopy to make qualitative purity assessments [20].

To conclusively test if the SWNT D-band intensity could be enhanced by defects as previously suggested [1,10], controlled oxidation reactions were performed to add defects to the purified materials. Purified SWNT samples were heated to temperatures between 1500 and 1650 °C for 15–120 min. within a tantalum foil in the minimum pressure that could be achieved at these high temperatures ($\sim 10^{-5}$ torr of H_2O). A significant weight loss was observed upon heating, and the higher temperature treatments caused the SWNT material to become more brittle. TEM indicated that the SWNTs had been significantly cut and damaged. The damage was greatest at the higher temperatures and longer times. For example, heating to 1650 °C for 60 min in $\sim 1 \times 10^{-5}$ torr H_2O was sufficient to destroy most of the SWNTs. TEM revealed that this material had transformed into significant quantities of graphitic and amorphous carbons, and Raman spectroscopy showed a significantly broadened D-band signal indicating the presence of non-nanotube carbon. For milder anneals, the intensity of the D-band relative to that of the G-band was observed to increase significantly while maintaining the same narrow D-band width. SWNTs heated to 1500 °C in $\sim 1 \times 10^{-5}$ torr H_2O lost weight but still retained their structure. The narrow D-band of the samples heated to 1500 °C suggested that none of the nanotubes were transformed to disordered carbon impurities [20], and this was further supported by extensive TEM analyses.

Fig. 2a displays high-resolution TEM images of the as-purified SWNTs. The bundle edges are continuous and no nanotube ends are apparent. Conversely, Fig. 2b shows damage in the SWNT bundles following heat treatments at 1500 °C in $\sim 1 \times 10^{-5}$ torr H_2O. Note now the edges of the bundles are quite ragged, and numerous nanotube ends are apparent. These and other TEM micrographs suggest that the damage appears uniform throughout the samples and the amount of damage increases with both time and temperature of the anneal. Also, significant damage is indicated by the TEM to tubes that are slightly larger than 1 nm, corresponding well with the diameter range probed at 2.54 eV excitation. Fig. 3 shows the Raman spectra between 1200 and 1800 cm^{-1} of an as-purified SWNT sample and the same sample following the introduction of defects by water oxidation at 1500 °C for 60 and 120 min with $E_{laser} = 2.54$ eV. An inset that magnifies the Raman D-band of these three samples is also shown in Fig. 3. All of the spectra were normalized to the intensity of

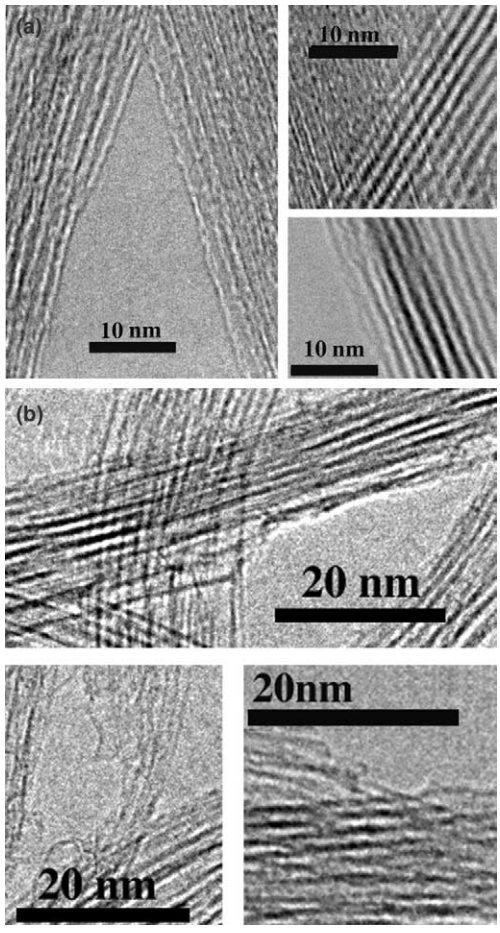

Fig. 2. High-resolution TEM images of (a) pristine bundles of purified laser generated SWNTs and (b) damaged purified SWNT structures following heat treatment for various times at 1500 °C in $\sim 10^{-5}$ torr H_2O.

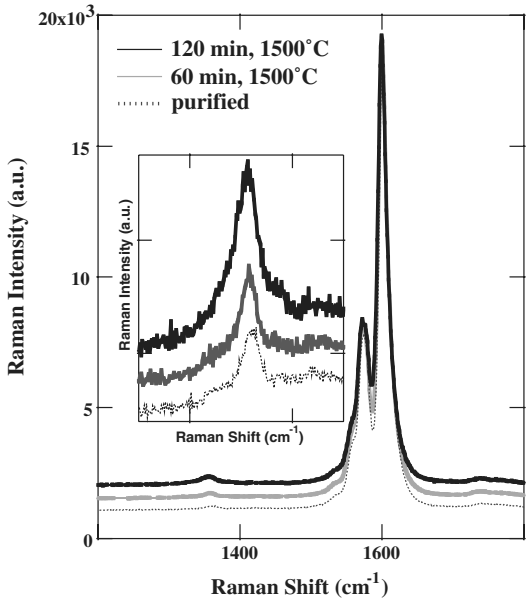

Fig. 3. Raman spectra taken with 2.54 eV excitation of purified laser-generated material and the same material heated to 1500 °C in $\sim 10^{-5}$ torr water vapor for 60 and 120 min. The inset shows the Raman spectra of the D-bands at an expanded scale.

the largest G-band so that relative changes in the D-band intensities are more easily observed. Although the D-band intensity is small relative to the G-band, it is still possible to observe a relative increase in the D-band intensity for the annealed samples to which defects have been introduced. Fig. 4a shows the D/G intensity ratio for purified samples that were heated to 1500 °C for varying lengths of time. In Fig. 4a it is apparent that the intensity of the D-band increases roughly linearly relative to the G-band with increasing reaction time as more defects are added to the SWNTs. The mean free path for water molecules at a pressure of $\sim 10^{-5}$ torr is on the order of 10 m, so the arrival of reactant to the SWNT substrate is mass-transport limited. Under these conditions, one expects the number of defects added to be linear with time. Thus, the approximately linear growth of the D/G ratio with time apparent in Fig. 4a is anticipated. The total increase in the D-band intensity is slightly less than a factor of two. The FWHMs of the D-bands for these samples are unchanged relative to the unheated starting material for heating times up to 120 min, as shown in Fig. 4b. The gradual introduction of defects, therefore, enhances the D-band intensity only slightly and does not broaden the SWNT D-band signal.

Fig. 4c shows the intensities of the D-band versus the G-band modes for ~60 different spectra obtained from samples produced under a variety of laser synthesis conditions (E_{laser} = 2.54 eV). The figure shows both as-purified samples (circles) and samples heated to temperatures ranging from 1000 to 1650 °C for times between

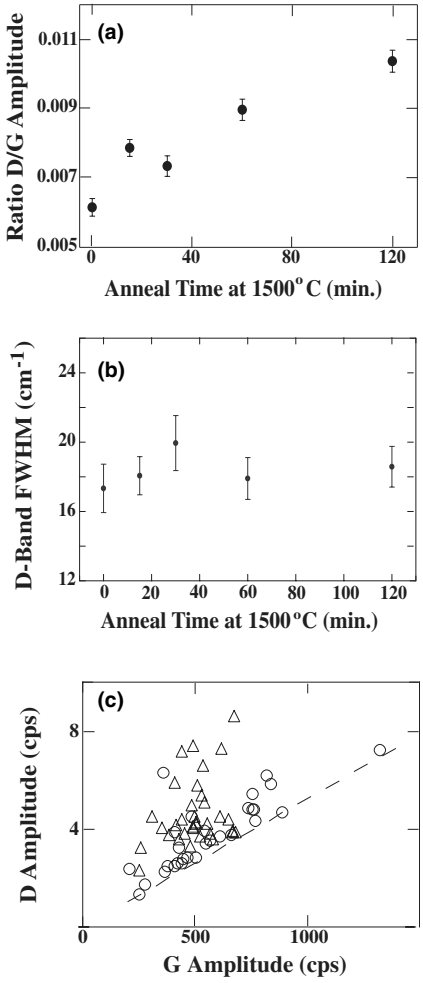

Fig. 4. (a) The D/G intensity ratio for several purified samples that were heated to 1500 °C for varying lengths of time in $\sim 1 \times 10^{-5}$ torr H_2O, (b) the FWHMs of the D-bands of these same samples and (c) the intensities of the D-band versus the G-band modes for ~60 spectra of both as-purified laser-generated samples (circles) and samples heated to temperatures ranging from 1000 to 1650 °C for times between 15 and 120 min (triangles). The dashed line below which none of the points fall is a guide to the eye.

15 and 120 min (triangles). The data shows a minimum D/G line below which none of the points fall (dashed line, Fig. 4c). Most of the data points lying far above this line are due to samples that were oxidized by heating in water. Annealed samples that are close to the line were annealed at the lower temperatures for shorter times and are therefore expected to have lower defect densities. The line is bordered mostly by points from as-purified, un-annealed samples. Some un-annealed samples are far from the line presumably because the particular synthesis/purification produced SWNTs with more defects.

The data from the annealing experiments are consistent with a gradual introduction of defects. The weight loss, the tubes becoming brittle and the TEM data show that oxidation and cutting are occurring spatially uni-

formly throughout the sample and in the extreme conditions, can destroy all the nanotubes. Given the endpoint that all tubes in these samples can be damaged by the annealing process, it is reasonable to expect that some damage occurs on all tubes at the milder conditions as well. Although it may be possible that the rate of defect introduction depends on tube chirality, the Raman data tracks a subset of the nanotubes in response to this defect introduction and a clear trend is observed. The results support using the D/G ratio as a method to make relative assessments of the number of defects in various purified nanotube samples. In comparing relative defect densities it will be important to look at samples with similar chirality distributions and to use the same laser excitation. It is also of course important to ensure that the samples are highly pure as the D-bands of most carbon impurities overlap the SWNT D-band. With further development and verification, it may even be possible to use the D/G ratio to quantitatively assess the defect density in pure nanotubes samples.

The existence of a minimum line corresponding to a D/G ratio of ~1/190 (Fig. 4c) suggests that the defect density is constant for the samples bordering this line. Since most of the data above the 1/190 line are from heated samples, the D/G ratio is evidently enhanced by the introduction of defects upon water oxidation. It appears that an approximately constant number of defects results from this particular laser-synthesis and purification technique (16 h reflux in HNO_3 followed by air oxidation at 550 °C [18]). Separate studies have confirmed that treating as-synthesized SWNTs in HNO_3 results in the introduction of new defects [23]. So the relatively constant D/G ratio of 1/190 for $E_{laser} = 2.54$ suggests that the production of these laser-generated tubes and the purification technique employed are very reproducible and introduce a relatively constant number of defects.

Since the intensities of the resonantly enhanced SWNT first order Raman modes vary with laser excitation, it is expected that the D/G ratio for the purified SWNTs studied here will also vary with laser excitation. It should, however, have a roughly constant value for each given laser excitation. To test this hypothesis, we examined purified SWNT samples with a Raman excitation of 1.96 eV. Fig. 5a compares the Raman spectra between 1200 and 1800 cm^{-1} for purified laser-generated SWNTs for Raman excitations of 2.54 and 1.96 eV. For excitation at 1.96 eV, a strong lower frequency G-band feature with a Breit–Wigner–Fano line shape is observed, consistent with resonance Raman of metallic SWNTs [24]. For most of the laser-generated materials in this study, this lower frequency G-band feature at 1537 cm^{-1} is slightly stronger than or approximately equal to the higher frequency tangential band at 1580 cm^{-1}. It is also evident in Fig. 5a that for Raman excitation at 1.96 eV, the intensity of the D-band relative to the G-bands is stronger than that observed at 2.54 eV excitation. Examination of eight purified SWNT samples with $E_{laser} = 1.96$ eV revealed a D/G ratio of ~1/40 with only one exception. Thus, although the relative D-band intensity is stronger for laser excitation of 1.96 eV, the roughly constant D/G ratio (1/40) again suggests that an approximately constant number of defects are introduced for the synthesis and purification techniques employed here.

The FWHM of the purified SWNT D-band observed for 1.96 eV excitation is also larger than that observed at 2.54 eV, 23 and 17 cm^{-1}, respectively. Fig. 5b compares Raman spectra of the RB modes of the purified laser-generated SWNTs for Raman excitation at 2.54 and 1.96 eV. The Raman spectra show SWNTs with diameters in the range of 1.2–1.5 nm and 1.3–2.3 nm for laser excitations of 2.54 and 1.96 eV, respectively [21,22]. The significantly broader diameter distribution observed for

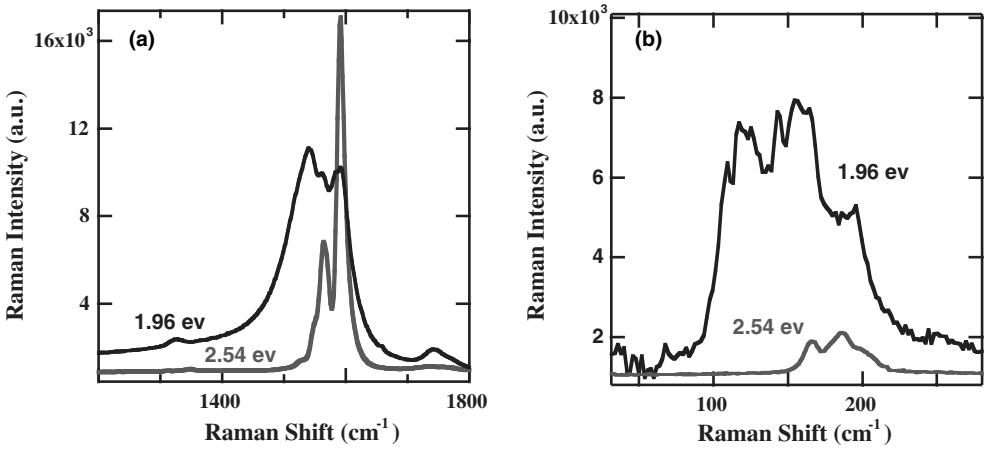

Fig. 5. Comparison of the Raman spectra of purified SWNTs acquired with 2.54 and 1.96 eV excitations for (a) the tangential and disorder induced vibration modes and (b) the RB modes.

E_{laser} = 1.96 eV explains why the FWHM of the D-band is 5 cm^{-1} larger than that observed at 2.54 eV, as it is consistent with the diameter dependent frequency of the SWNT D-band [10].

4. Conclusions

We have experimentally demonstrated that the Raman intensity of the SWNT D-band in pure, bulk SWNT samples is defect-activated. A slight increase in the D-band intensity is observed relative to the intensity of the G-band when a small number of defects are introduced, but the SWNT structural integrity is maintained. When a gentle mass-transport-limited oxidation reaction is employed to introduce defects, the Raman D-band intensity increases approximately linearly with reaction time. Also a roughly constant value for the D/G Raman intensity ratio for purified samples prior to heat treatments to introduce defects was found to be 1/190 and 1/40 for 2.54 and 1.96 eV excitation, respectively. Further in-depth Raman studies for SWNT materials prepared by different synthesis and purification techniques are required to determine whether a similar constant D/G intensity ratio exists.

Acknowledgements

This work was funded by the US Department of Energy Office of Energy Efficiency and Renewable Energy and by the Office of Science, Basic Energy Sciences, Materials Sciences and Engineering under subcontract DE-AC36-99GO10337 to NREL.

References

[1] R. Saito, G. Dresselhaus, M. Dresselhaus, Physical Properties of Carbon Nanotubes, Imperial College Press, 1998.
[2] A.M. Rao, E. Richter, S. Bandow, B. Chase, P.C. Eklund, K.A. Williams, S. Fang, K.R. Subbaswamy, M. Menon, A. Thess, R.E. Smalley, G. Dresselhaus, M.S. Dresselhaus, Science 275 (1997) 187.
[3] H. Kataura, Y. Kumazawa, Y. Maniwa, I. Umezu, S. Suzuki, Y. Ohtsuka, Y. Achiba, Synth. Met. 103 (1999) 2555.
[4] R. Saito, G. Dresselhaus, M.S. Dresselhaus, Phys. Rev. B 61 (2000) 2981.
[5] S.D.M. Brown, P. Corio, A. Marucci, M.A. Pimenta, M.S. Dresselhaus, G. Dresselhaus, Phys. Rev. B 61 (2000) 7734.
[6] R. Saito, A. Jorio, A.G. Souza Filho, G. Dresselhaus, M.S. Dresselhaus, A. Gruneis, L.G. Cancado, M.A. Pimenta, Jpn. J. Appl. Phys. 41 (2002) 4878.
[7] M.A. Pimenta, E.B. Hanlon, A. Marucci, P. Corio, S.D.M. Brown, S.A. Empedocles, M.G. Bawendi, G. Dresselhaus, M.S. Dresselhaus, Braz. J. Phys. 30 (2000) 423.
[8] R. Saito, T. Takeya, T. Kimura, G. Dresselhaus, M.S. Dresselhaus, Phys. Rev. B 57 (1998) 4145.
[9] G.S. Duesberg, I. Loa, M. Burghard, K. Syassen, S. Roth, Phys. Rev. Lett. 85 (2000) 5436.
[10] M.A. Pimenta, A. Jorio, D.M. Brown, A.G. Souza Filho, G. Dresselhaus, J.H. Hafner, C.M. Lieber, R. Saito, M.S. Dresselhaus, Phys. Rev. B 64 (2001) 041401.
[11] V. Zolyomi, J. Kurti, Phys. Rev. B 66 (2002) 073418.
[12] C. Thomsen, S. Reich, Phys. Rev. Lett. 85 (2000) 5214.
[13] R. Saito, A. Jorio, A.G. Souza Filho, G. Dresselhaus, M.S. Dresselhaus, M.A. Pimenta, Phys. Rev. Lett. 88 (2002) 027401.
[14] J. Kurti, V. Zolyomi, A. Gruneis, H. Kuzmany, Phys. Rev. B 65 (2002) 165433.
[15] V. Zolyomi, J. Kurti, A. Gruneis, H. Kuzamany, Phys. Rev. Lett. 90 (2003) 157401.
[16] A.G. Souza Filho, A. Jorio, G.G. Samsonidze, G. Dresselhaus, R. Saito, M.S. Dresselhaus, Nanotechnology 14 (2003) 1130.
[17] J.L. Bahr, J. Yang, V. Kosynkin, M.J. Bronikowski, R.E. Smalley, J.M. Tour, J. Am. Chem. Soc. 123 (2001) 6536.
[18] A.C. Dillon, T. Gennett, K.M. Jones, J.L. Alleman, P.A. Parilla, M.J. Heben, Adv. Mat. 11 (1999) 1354.
[19] A.C. Dillon, P.A. Parilla, J.L. Alleman, J.D. Perkins, M.J. Heben, Chem. Phys. Lett. 316 (2000) 13.
[20] A.C. Dillon, M. Yudasaka, M.S. Dresselhaus, J. Nanosci. Nanotech. 407 (2004) 691.
[21] S. Bandow, S. Asaka, Y. Saito, A.M. Rao, L. Grigorian, E. Richter, P.C. Eklund, Phys. Rev. Lett. 80 (1998) 3779.
[22] A. Kukovecz, C. Kramberger, V. Georgakilas, M. Prato, H. Kuzmany, Eur. Phys. J. B 28 (2002) 223.
[23] H. Hui, B. Zhao, M.E. Itkis, R.C. Haddon, J. Phys. Chem. B 107 (2003) 13838.
[24] S.D.M. Brown, A. Jorio, P. Corio, M.S. Dresselhaus, G. Dresselhaus, R. Saito, K. Kneipp, Phys. Rev. B 63 (2001) 155414.